



Available online at  
**ScienceDirect**  
www.sciencedirect.com

Elsevier Masson France  
**EM|consulte**  
www.em-consulte.com/en



CLINICAL RESEARCH

## Cardiovascular anatomy in children with bidirectional Glenn anastomosis, regarding the transcatheter Fontan completion

*Anatomie cardiovasculaire chez les enfants avec de la dérivation cavopulmonaire partielle concernant l'achèvement de la dérivation cavopulmonaire totale par voie percutanée*

Aleksander Sizarov<sup>a</sup>, Francesca Raimondi<sup>a,b</sup>, Damien Bonnet<sup>a,c</sup>, Younes Boudjemline<sup>a,c,\*</sup>

<sup>a</sup> Service de cardiologie pédiatrique, centre de référence malformations cardiaques congénitales complexes – M3C, hôpital universitaire Necker-Enfants-Malades, Assistance publique–Hôpitaux de Paris, 149, rue de Sèvres, 75015 Paris cedex, France

<sup>b</sup> Service de radiologie pédiatrique, hôpital universitaire Necker-Enfants-Malades, Assistance publique–Hôpitaux de Paris, 75015 Paris, France

<sup>c</sup> Université Paris V Descartes, 75006 Paris, France

Received 27 March 2017; received in revised form 14 May 2017; accepted 7 August 2017

### KEYWORDS

Cardiac computed tomography;  
Cardiac magnetic resonance imaging;  
Congenital heart disease;  
Transcatheter Fontan completion

### Summary

**Background.** – Transcatheter stent-secured completion of total cavopulmonary connection (TCPC) after surgical preparations during the Glenn anastomosis procedure has been reported, but complications from this approach have precluded its clinical acceptance.

**Aims.** – To analyse cardiovascular morphology and dimensions in children with bidirectional Glenn anastomosis, regarding the optimal device design for transcatheter Fontan completion without special surgical “preconditionings”.

**Methods.** – We retrospectively analysed 60 thoracic computed tomography and magnetic resonance angiograms performed in patients with a median age of 4.1 years (range: 1.8–17.1 years). Additionally, we simulated TCPC completion using different intra-atrial stent-grafts in a three-dimensional model of the representative anatomy, and performed calculations to determine the optimal stent-graft dimensions, using measured distances.

**Abbreviations:** 3D, Three-dimensional; IVC, Inferior vena cava; PA, Pulmonary artery; RPA, Right pulmonary artery; RUPV, Right upper pulmonary vein; SVC, Superior vena cava; TCPC, Total cavopulmonary connection.

\* Corresponding author. Service de cardiologie pédiatrique, centre de référence malformations cardiaques congénitales complexes – M3C, hôpital universitaire Necker-Enfants-Malades, Assistance publique–Hôpitaux de Paris, 149, rue de Sèvres, 75015 Paris cedex, France.

E-mail address: [yboudjemline@yahoo.fr](mailto:yboudjemline@yahoo.fr) (Y. Boudjemline).

<https://doi.org/10.1016/j.acvd.2017.08.003>

1875-2136/© 2017 Elsevier Masson SAS. All rights reserved.

Please cite this article in press as: Sizarov A, et al. Cardiovascular anatomy in children with bidirectional Glenn anastomosis, regarding the transcatheter Fontan completion. Arch Cardiovasc Dis (2017), <https://doi.org/10.1016/j.acvd.2017.08.003>

**Results.** – Two types of cardiovascular arrangement were identified: left atrium interposing between the right pulmonary artery (RPA) and inferior vena cava, with the right upper pulmonary vein (RUPV) orifice close to the intercaval axis (65%); and intercaval axis traversing only the right(-sided) atrial cavity, with the RUPV located posterior to the atrial wall (35%). In the total population, the shortest median RPA-to-atrial wall distance was 1.9 mm (range: 0.6–13.8 mm), while the mean intra-atrial distance along the intercaval axis was  $50.1 \pm 11.2$  mm. Regardless of the arrangement, 83% of all patients required a deviation of at least  $5.9 \pm 2.4$  mm (range: 1.2–12.7 mm) of the stent-graft centre at the RUPV level anteriorly to the intercaval axis to avoid covering or compressing this vein. Fixing the anterior deviation of the curved stent-graft centre at 10 mm significantly decreased the range of bend angle per every given RUPV-RPA distance.

**Conclusions.** – For both types of cardiovascular arrangement, after conventional bidirectional Glenn anastomosis, the intra-atrial curved stent-graft seemed most suitable for achieving uncomplicated TCPC completion percutaneously without previous surgical ‘‘preconditionings’’ in the majority of children. Experimental study is necessary to validate this conclusion.

© 2017 Elsevier Masson SAS. All rights reserved.

## MOTS CLÉS

Scanner cardiaque ;  
Imagerie par  
résonance  
magnétique  
cardiaque ;  
Cardiopathies  
congénitales ;  
Dérivation  
cavopulmonaire  
totale (Fontan) ;  
Totalisation de  
Fontan par voie  
percutanée

## Résumé

**Contexte.** – La totalisation de la dérivation cavopulmonaire partielle (DCP) par voie percutanée après préparation chirurgicale a été rapportée. Cependant, les complications résultantes de cette approche ont empêché son acceptation par tous.

**Objectifs.** – Le but de l'étude est de caractériser l'anatomie cardiovasculaire chez les enfants ayant une dérivation cavopulmonaire partielle et d'en déduire le design optimal d'un dispositif dans l'optique d'une totalisation d'une DCP par voie percutanée sans préconditionnement.

**Méthodes.** – Nous avons analysé rétrospectivement 60 scanners et imageries par résonance magnétique thoraciques réalisés à un âge moyen de  $5,5 \pm 3,4$  ans. Nous avons simulé la totalisation d'un DCP par différents stents dans un modèle anatomique tridimensionnel.

**Résultats.** – Deux types d'arrangement ont été identifiés : (1) l'oreillette gauche s'interposant entre l'artère pulmonaire droite (APD) et la veine cave inférieure (VCI) avec l'orifice de la veine pulmonaire supérieure droite (VPSD) près de l'axe intercaval (65 %) ; (2) l'axe intercave traversant seulement l'oreillette droite avec VPSD localisé postérieur à la paroi auriculaire (35 %). Dans la population totale, la distance médiane la plus courte entre l'APD à l'oreillette était de 1,9 mm (0,6–13,8 mm). La distance moyenne intra-auriculaire le long de l'axe intercave était de  $50,1 \pm 11,2$  mm. Quel que soit l'arrangement, 83 % des patients nécessiteraient une déviation antérieure de  $5,9 \pm 2,4$  mm (1,2–12,7 mm) du centre du stent au niveau de la VPSD avant l'axe intercave afin d'éviter de couvrir ou de comprimer cette veine.

**Conclusions.** – Pour les deux types de l'arrangement cardiovasculaire après la dérivation cavopulmonaire partielle conventionnelle, une endoprothèse vasculaire courbée semble la plus appropriée pour totaliser une DCP par voie percutanée sans « préconditionnement » chirurgical préalable chez la grande majorité des enfants. Une étude expérimentale est nécessaire pour valider cette conclusion.

© 2017 Elsevier Masson SAS. Tous droits réservés.

## Background

Patients with congenital heart defects, where biventricular repair is unfeasible, undergo multiple cardiothoracic surgical procedures, with the final intervention usually being total cavopulmonary connection (TCPC) completion. Extracardiac TCPC modification using a polymeric conduit to connect the inferior vena cava (IVC) to the right pulmonary artery (RPA) has become a standard approach for all types of univentricular heart lesions [1]. Although it is a relatively

simple procedure technically, the surgical insertion of an extracardiac conduit to complete the TCPC demands extensive intrathoracic exploration, often using cardiopulmonary bypass. Although a very low mortality rate is currently achieved after extracardiac TCPC completion, this procedure may be associated with considerable morbidity [1,2]. While this morbidity largely relates to slow or absent circulation adaptation to passive blood flow through the pulmonary vasculature in some patients, the adverse effects of chest opening and cardiopulmonary bypass also play a role [3].

Transcatheter TCPC completion would allow faster post-procedural recovery and ventricular function preservation, by obviating the need for sternotomy and cardiopulmonary bypass. Many attempts have been made to modify the bidirectional Glenn anastomosis or hemi-Fontan procedures, to prepare a foothold for transcatheter TCPC completion [4–11]. None of these surgical “preconditionings” has been accepted clinically, because of several adverse issues. Most importantly, any surgical “preconditioning” performed in young infants produces a complication-prone situation for several years before the TCPC completion becomes clinically indicated [12].

Here, we sought to analyse tomographic cardiovascular imaging performed in children after conventional bidirectional Glenn anastomosis, regarding the design of a dedicated device for transcatheter Fontan completion without special surgical “preconditionings”.

## Methods

### Patients

We reviewed the database of our institution (Necker hospital for sick children, Paris, France) to identify the patients who underwent computed tomography or magnetic resonance imaging angiography after the Glenn procedure, and before TCPC completion, in 2006 to 2015. A variety of contrast medium doses and injection timings were used over the years. Patients were excluded if they were aged < 1.5 years at the time of the scan or had an interrupted IVC, an unrepaired anomalous pulmonary venous connection of the extracardiac type, discontinued pulmonary artery (PA) branches or incompletely visualized cardiovascular anatomy.

### Morphometric measurements

A covered stent-graft with a diameter of 18–20 mm, deployed between the distal IVC and the PA branch, will constitute a dedicated transcatheter TCPC completion device. Analysis of cardiovascular morphology and morphometric measurements considered as important for device design were performed for all included patients, independent of eventual suitability for the procedure in the clinical setting. To standardize the measurements, manipulations of the planes through the scans were limited to the following steps. Oblique sagittal and coronal orthogonal planes were produced along the line passing through the centres of the Glenn anastomosis and the IVC-to-right atrial junction, defined here as the intercaval axis (Fig. 1). Then, an axial plane through the orifice of the right upper pulmonary vein (RUPV) was produced without altering the other planes. The RUPV orifice position relative to the intercaval axis, and the presence of the atrial wall between the axis and RUPV, were used to determine the cardiovascular arrangement type. In patients with bilateral Glenn anastomoses, the planes through the right-sided connection were used. Measurements were performed on resultant planes as outlined in Fig. 1. To determine intra- and interobserver variability, measurements were repeated on 11 randomly selected scans by two investigators, independently (A. S. and F. R.).

### Simulation of TCPC completing device and calculation of its dimensions

To illustrate the representative spatial relationship between the Glenn anastomosis, atrial cavities and right-sided pulmonary veins regarding the stent-secured TCPC completion, a three-dimensional (3D) model of the related vessels and parts of the atria was prepared. Using serial images from a thoracic computed tomography angiogram of a child with bidirectional Glenn anastomosis, pulmonary valve atresia and right ventricular hypoplasia, label-fields of the walls were created manually for the anastomosed superior vena cava (SVC) and PA branches (coloured purple), the right atrium and the distal IVC (blue), and the right-sided left atrium part and pulmonary veins (orange), in the 3D reconstruction software Amira 5.2 (Thermo Fisher Scientific, Waltham, MA, USA). After correcting deformities of the label-fields, a 3D surface was generated, simplified and further smoothed to obtain the final 3D model.

Using anatomical landmarks, a wall of hypothetically suitable 18 mm intra-atrial stent-graft (coloured gray) was superimposed on the previously created label-fields. Two graft types were simulated: straight (i.e. with its centre along the intercaval axis); and curved at the cranial end (i.e. with its centre deviated anteriorly to the intercaval axis). To increase the safety margin of future clinical applications, the optimal dimensions of the curved intra-atrial device to avoid covering or compressing of RUPV were calculated using the measured distances, as outlined in Fig. A.1, for patients where a larger (20 mm) straight intra-atrial covered stent-graft would compromise this vein.

### Statistical analysis

Normality of distribution was assessed using the  $\chi^2$  goodness-of-fit test. Means  $\pm$  standard deviations or medians [interquartile ranges] were calculated where appropriate. Differences between the samples were tested using Student’s *t*-distribution two-tailed test or the  $\chi^2$  test for proportions. Correlation between two variables was assessed using Pearson’s coefficient of determination. A *P*-value < 0.05 was considered significant.

## Results

### Clinical data

We analysed 60 thoracic tomographic angiograms (47 computed tomography and 13 magnetic resonance imaging scans), providing anatomical visualization sufficient for intended measurements, and performed  $3.9 \pm 2.6$  years (range: 0.4–12.3 years) after a bidirectional Glenn procedure in patients with various types of univentricular heart defects. The median age of the patients at the time of the scan was 4.1 years (range: 1.8–17.1 years); 39 patients (65%) were aged < 5 years. In total, 16 scans did not meet the inclusion criteria.

Before the Glenn procedure, 78% of the patients underwent initial surgical palliation (Norwood procedure, systemic-to-PA shunts, PA banding), while 70% of the

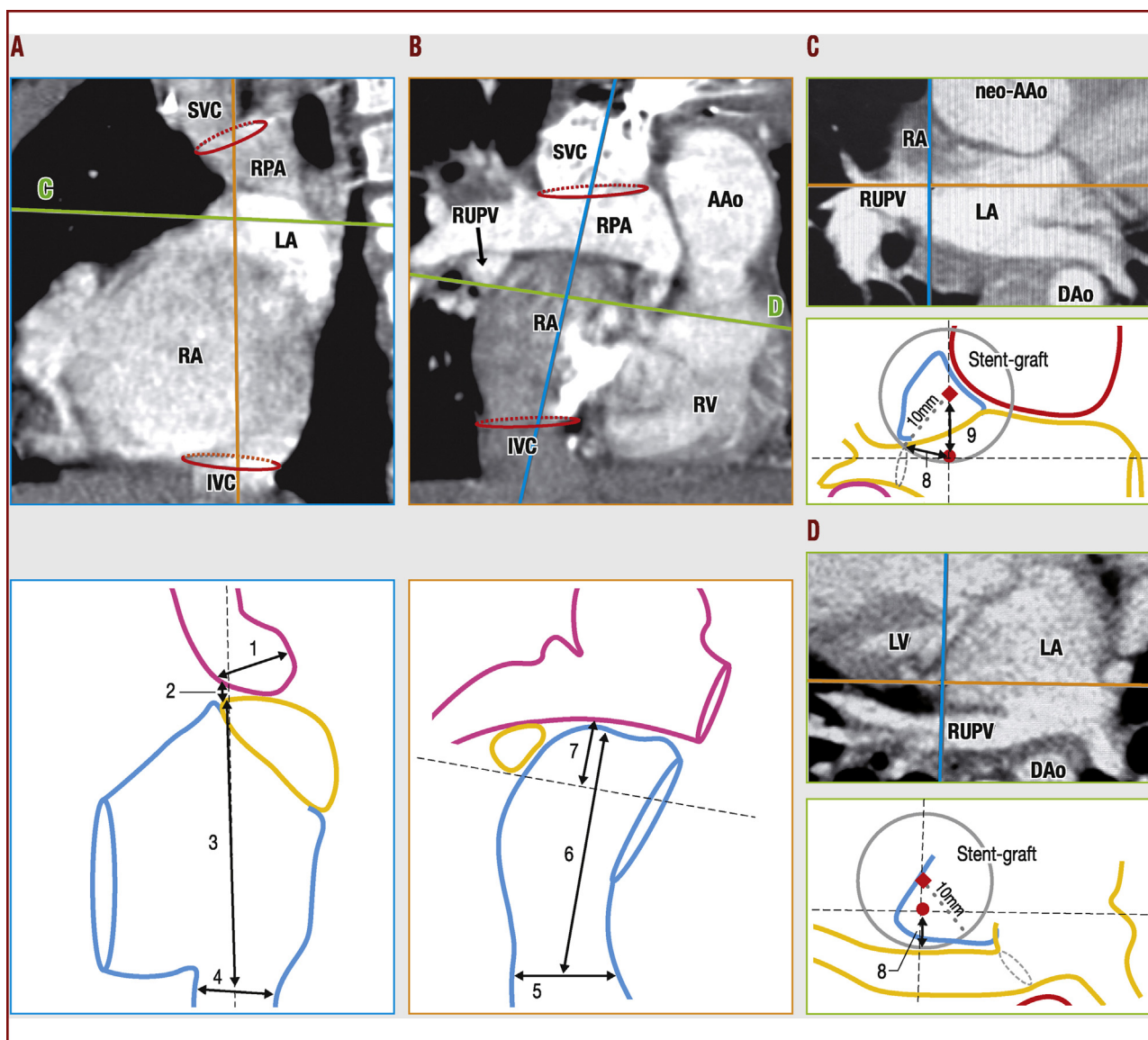


**Figure 1.** Definition of morphometric measurements. A–D. Computed tomography scan sections in two different patients, with and without left atrium (LA) interposition between the Glenn anastomosis and the distal inferior vena cava (IVC). Oblique sagittal and coronal planes transect the centres of the Glenn anastomosis and the right atrium (RA)-to-IVC junction (red circles). Axial planes through the right upper pulmonary vein (RUPV) orifice (indicated by green line in panels A and B). Corresponding schematic drawings below the computed tomography sections show performed measurements by numbers: (1) right pulmonary artery (RPA) diameter below the Glenn anastomosis; (4, 5) IVC diameter; (2) shortest distance from RPA to adjacent atrial wall; (3, 6) longitudinal distance within the atria along the intercaval axis; (7) distance from RPA caudal surface to RUPV orifice level; (8) distance from intercaval axis (red dots in panels C and D) to nearest RUPV part. The position of the RUPV orifice (dashed ellipses) relative to the intercaval axis determined the type of cardiovascular arrangement (see text). Anterior deviation of the 20 mm centre of the stent-graft (diamonds in panels C and D), necessary to avoid RUPV compromise, depending on the type, was either measured in the axial plane (9 in panel C) or calculated by subtraction. Aao: ascending aorta; Dao: descending aorta; LV: left ventricle; RV: right ventricle; SVC: superior vena cava.

patients received various additional surgical procedures concomitant with the Glenn shunt (systemic-to-PA shunt removal, patch-plasty of hypoplastic PAs or Damus-Kaye-Stansel anastomosis). After the scan, 85% of the children underwent TCPC completion, with all but two having an extracardiac conduit (mean diameter 18 mm). Twenty-nine percent had indications for concomitant surgical interventions during the TCPC completion (i.e. atrioseptectomy, PA patch-plasty, removal of the shunts or stents or atrioventricular valve repair).

### Morphology of the intercaval region

Two types of cardiovascular arrangement were identified, based on the relationship between the intercaval axis and the pulmonary venous return. Thirty-nine scans (65%), designated type 1 arrangement, demonstrated left atrial cavity interposition between the Glenn anastomosis and the IVC, with the RUPV orifice locating mostly within a 10-mm distance from the intercaval axis (Fig. 2). Twenty-one scans (35%), designated type 2 arrangement, showed the

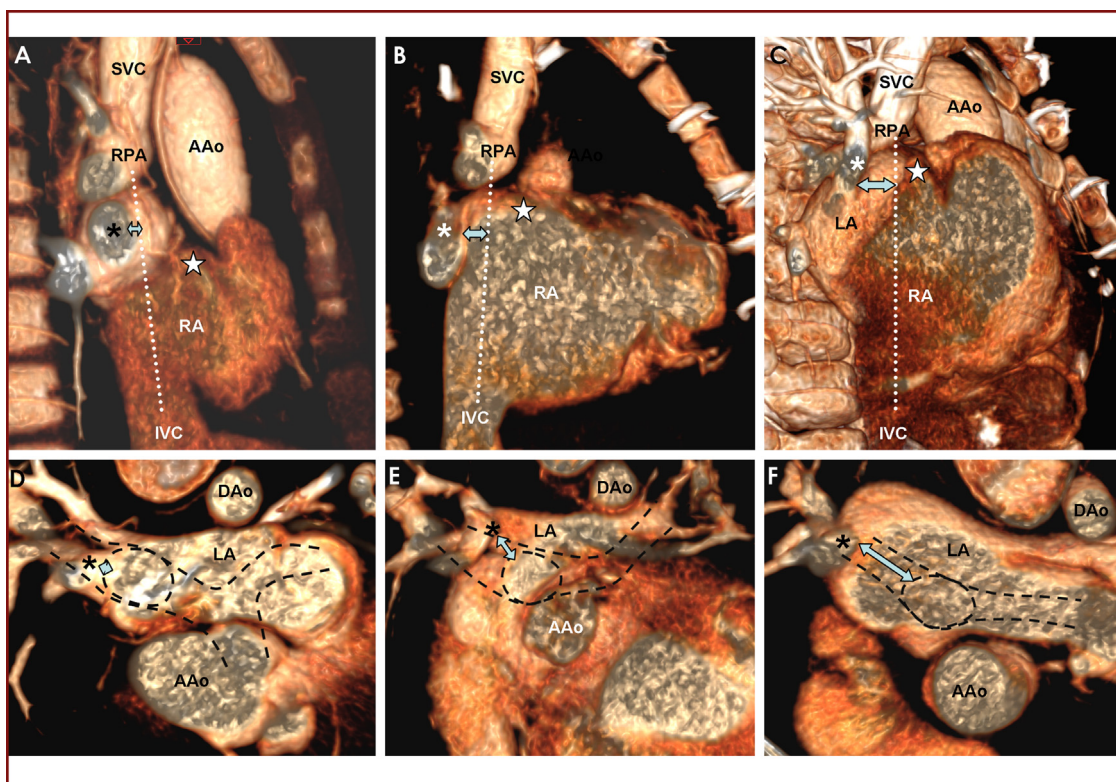


**Figure 2.** Intercaval region in type 1 cardiovascular arrangement. Right lateral views (panels A–C) and cranial views (panels D–F) of the maximum intensity projections are shown. Dotted lines in panels A–C represent the intercaval axis; superimposed dashed lines in panels D–F represent contour projections of the more cranially located pulmonary arteries and Glenn anastomosis. Asterisks point to the right upper pulmonary artery (RUPV). Note the varying distance between the Glenn anastomosis and the distal RUPV (double arrows). Note also the substantial gap between the right pulmonary artery (RPA) caudal surface and the nearest part of the right atrium (RA) (star). Aao: ascending aorta; Dao: descending aorta; IVC: inferior vena cava; LA: left atrium; SVC: superior vena cava.

intercaval axis traversing only the right(-sided) atrial cavity, with the distal RUPV lumen being posterior to the atrial wall (Fig. 3). The age of the patients with each type of arrangement was nearly identical. Among the two types, the presence of all univentricular heart defects was very similar, except for hypoplastic left heart syndrome, which was identified only in patients with the type 1 arrangement.

In all patients but three, the caudal surface of the RPA below the Glenn anastomosis was in tight contact with or within a 5-mm distance of the cranial aspect of adjacent atrium. In the total population, the shortest median RPA-to-atrial wall distance was 1.9 mm (range: 0.6–13.8 mm). The space between these two compartments was filled with mediastinal tissue only. On 45% of the scans, the stump of the distal SVC was clearly visible in the vicinity of the RPA caudal surface below the Glenn anastomosis, while on 42% of the scans, an atrial septum – with or without small defect – was present. As expected, the atrial septum was more prevalent in the type 2 arrangement (71% vs 31% in type 1;  $P=0.003$ ). The RPA-to-atrium tightest contact area was bordered anteriorly by lung tissue (in 32% of patients), the root of the ascending aorta or pulmonary trunk (in 33%), the right atrial appendage (in 25%) or mediastinal tissue. Posteriorly, the contact area was bordered by mediastinal tissue in the majority of the patients.

### Morphometry of the intercaval region

Results of morphometric measurements are summarized in Table 1. Except for single extreme outliers in some measurements, values showed a normal distribution. To increase the safety margin of future applications, a cut-off value of 10 mm, which is half the diameter of the larger conduit size currently used in the clinical setting, was applied in assessing potential mismatches between the measured distances and the eventual TCPC completion device. Ninety-five percent of patients aged < 5 years, and 83% of the whole population, had an RPA diameter below the Glenn anastomosis of < 20 mm, potentially resulting in a mismatch with the round stent end deployed through the RPA wall. Curved form and tortuous course of the adjacent PA and atrial walls have precluded accurate assessment of their contact extension beyond the intercaval axis. Within the atria, the longitudinal distance along the intercaval axis had a weak, but significant, positive correlation with age ( $r^2=0.37$ ;  $P<0.01$ ). In contrast, the distance between the RPA caudal surface and the RUPV orifice level varied widely among patients, and did not correlate with age ( $r^2=0.024$ ;  $P=0.24$ ), but with longitudinal atrial length ( $r^2=0.255$ ;  $P<0.01$ ).

In total, one-third of patients had an RUPV-RPA distance < 10 mm, resulting in potential covering of the RUPV orifice by the cranial aspect of the round 20 mm stent-graft

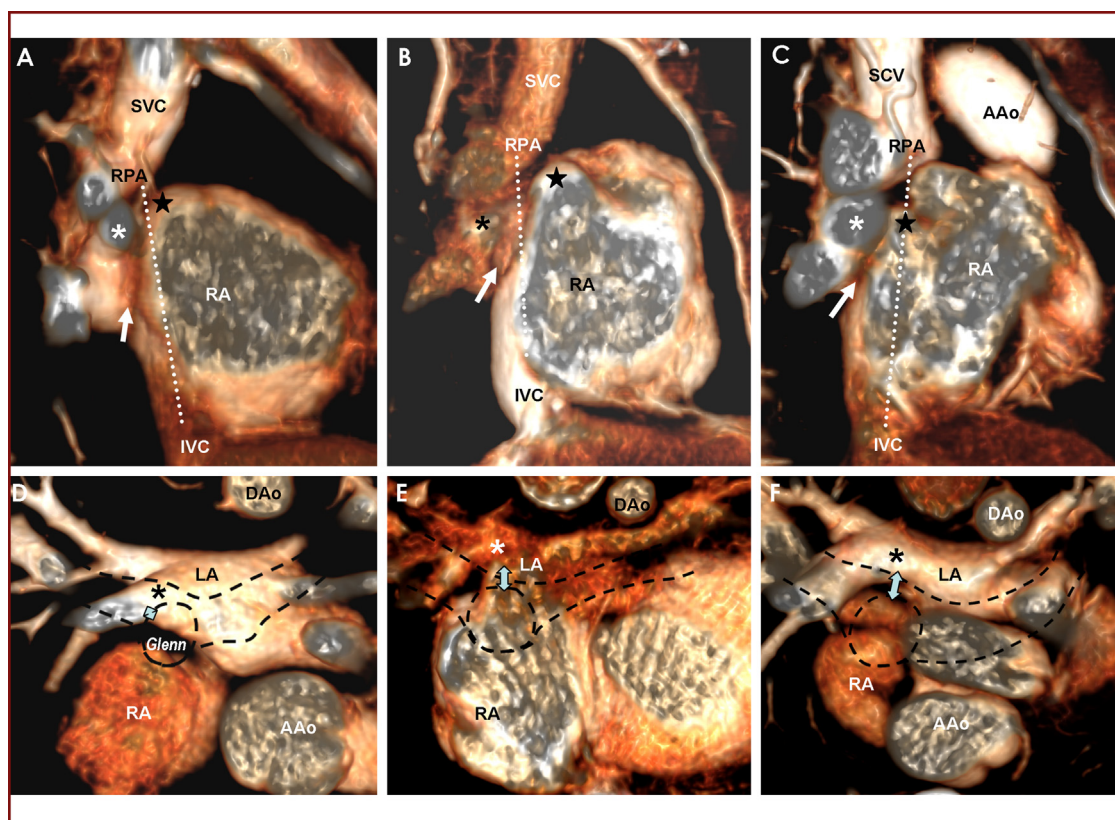


**Figure 3.** Intercaval region in type 2 cardiovascular arrangement. Right lateral views (panels A–C) and cranial views (panels D–F) of the maximum intensity projections are shown. Dotted lines in panels A–C represent the intercaval axis, and the stars point to the nearest part of right atrium (RA); superimposed dashed lines in panels D–F represent contour projections of the more cranially located pulmonary arteries and Glenn anastomosis. Asterisks point to the distal right upper pulmonary vein (RUPV), while double arrows point to the variable distance between the Glenn anastomosis and the RUPV. Note the left atrial (LA) cavity and RUPV located posterior to the Glenn anastomosis, and the “groove” (arrows in panels A–C) corresponding to the atrial wall and/or extracardiac tissue separating the pulmonary venous lumens from the RA. Aao: ascending aorta; Dao: descending aorta; IVC: inferior vena cava; LA: left atrium; RPA: right pulmonary artery; SVC: superior vena cava.

deployed through the adjacent RPA and atrial walls. In patients with the type 1 arrangement, the RUPV orifice border nearest to the intercaval axis (i.e. the centre of the eventual straight stent-graft) was at a mean distance of  $7.7 \pm 4.2$  mm (range: 1–20.1 mm), with only seven patients having it at a distance of  $\geq 10$  mm. In patients with the type 2 arrangement, the mean shortest distance between the intercaval axis and the nearest RUPV part was  $5.6 \pm 2.8$  mm (range: 1.3–12.4 mm), with only three patients having a distance  $\geq 10$  mm. Thus, regardless of the anatomical arrangement type, in 83% of the whole population and 82% of those aged  $< 5$  years, placement of an intra-atrial straight 20 mm stent-graft would result in either covering or compression of the RUPV (Fig. 4A and B).

In all patients, the cross-section of the IVC at its junction with the right atrium had an elliptical shape. Twenty-eight percent of patients aged  $< 5$  years, and 37% of the whole population, had an average IVC diameter  $> 20$  mm, potentially resulting in incomplete sealing of the straight device. The majority of patients had only weak contrasting of the hepatic veins. For patients where measurement of the distance between the hepatic venous confluence and the right atrium-to-IVC junction was possible, it constituted  $7.0 \pm 2.5$  mm (range: 3–14.5 mm), thus giving an estimation

of the relatively short landing zone for the device within the distal IVC.

### Calculated dimensions of the dedicated stent-graft

In the total population, 83% of all patients would require a deviation of at least  $5.9 \pm 2.4$  mm (range: 1.2–12.7 mm) of the stent-graft centre at the RUPV level anteriorly to the intercaval axis to avoid covering or compressing this vein. In patients with the type 1 arrangement, a deviation of the stent-graft centreline at the RUPV level anteriorly by at least  $6.3 \pm 2.6$  mm (range: 1.2–12.7) would be needed to allow placement of a 20-mm covered graft without obstructing the RUPV orifice. Similarly, in patients with the type 2 arrangement, an anterior deviation of the stent-graft centreline by at least  $5.3 \pm 1.9$  mm (range: 1.8–8.7) would be necessary to avoid RUPV compression. In all patients but one, the extent of this deviation was  $\leq 10$  mm. Stent-graft deviation is achievable through a curvature at its cranial aspect, with the maximal extension at the RUPV level, producing shorter upper and longer lower arcs of the device reaching into the RPA and IVC, respectively (Fig. 4C and D).

**Table 1** Morphometric data.

	Patients aged < 5 years (n = 39)	Patients aged ≥ 5 years (n = 21)	Whole population (n = 60)	Intra-/interobserver variability (%) <sup>c</sup>
RPA diameter (mm) <sup>a</sup>	12.2 [10.4–13.9] (7.8–22.3)	16.0 [12.2–20.1] (10–32.9)	13.6 [11.4–16.0] (7.8–32.9)	5.0 ± 4.3/11.2 ± 10.6
Mean IVC diameter (mm) <sup>b</sup>	18.4 ± 3.2 (12.8–24.2)	22.0 ± 4.6 (15.8–31.1)	19.7 ± 4.0 (12.8–31.1)	7.8 ± 7.9/11.0 ± 10.6
Shortest distance from RPA to atrial wall (mm) <sup>a</sup>	1.7 [1.2–2.7] (0.6–9.3)	2.5 [1.1–3.8] (0.7–13.8)	1.9 [1.1–3.2] (0.6–13.8)	30.1 ± 18.1/20.2 ± 15.1
Average longitudinal intra-atrial distance (mm) <sup>b</sup>	45.3 ± 7.0 (34–63)	58.0 ± 13.0 (38–81)	50.1 ± 11.2 (34–81)	5.2 ± 4.0/5.8 ± 3.8
Distance from RPA to RUPV orifice level (mm) <sup>b</sup>	11.4 ± 4.1 (5.0–21.4)	12.7 ± 5.0 (5.1–25.9)	11.9 ± 4.4 (5.0–25.9)	12.2 ± 13.1/18.2 ± 15.5
Distance from intercaval axis to nearest RUPV border (mm) <sup>a</sup>	6.3 [4.5–7.9] (1.3–19.6)	6.3 [4.9–7.6] (1.0–20.1)	6.4 [4.5–8.0] (1.0–20.1)	10.0 ± 7.0/10.5 ± 11.1

IVC: inferior vena cava; RPA: right pulmonary artery; RUPV: right upper pulmonary vein.

<sup>a</sup> Variables with single extreme outliers in the range of values, causing skewed distribution, expressed as median [interquartile range] (range of minimum–maximum values).

<sup>b</sup> Variables with normal distribution of values, expressed as mean ± standard deviation (range of minimum–maximum values).

<sup>c</sup> Intra- and interobserver variabilities were calculated as the difference between the two sets of the same variable measurements divided by their mean, shown as a percentage, and expressed as mean ± standard deviation.

**Table 2** Centreline parameters of the curved stent-graft, calculated using measured distances<sup>a</sup>.

	Patients aged < 5 years (n = 32)		Whole population (n = 50)	
	Measured anterior deviation	At 10 mm fixed deviation	Measured anterior deviation	At 10 mm fixed deviation
Total length (mm)	47.8 ± 6.3 (37.0–67.1)	51.6 ± 5.8 (41.9–69.2)	51.4 ± 9.8 (37.0–82.3)	55.3 ± 9.5 (41.9–84.7)
Measured anterior deviation (mm)	6.2 ± 2.4 (1.8–12.7)	–	5.9 ± 2.4 (1.2–12.7)	–
Upper arc length (mm)	13.4 ± 3.1 (8.1–20.1)	16.0 ± 2.9 (11.6–22.9)	13.6 ± 3.7 (6.8–26.5)	16.3 ± 3.3 (11.6–28.4)
Lower arc length (mm)	34.5 ± 5.2 (24.4–51.7)	35.6 ± 5.0 (26.1–52.2)	37.9 ± 8.9 (24.4–66.7)	38.9 ± 8.7 (26.1–67.6)
Ratio of lower to upper arc lengths	2.7 ± 0.7 (1.8–4.0)	2.3 ± 0.5 (1.6–3.2)	3.0 ± 1.2 (1.7–7.5)	2.5 ± 0.7 (1.5–4.8)
Bend angle (°)	138.1 ± 17.9 (97–169)	118.5 ± 10.0 (99–137)	140.7 ± 17.3 (97–174)	120.4 ± 10.5 (99–149)

Data are expressed as mean ± standard deviation (range of minimum–maximum values).  
<sup>a</sup> See [Fig. A.1](#) online for outline of calculations and dimensions shown in this table.



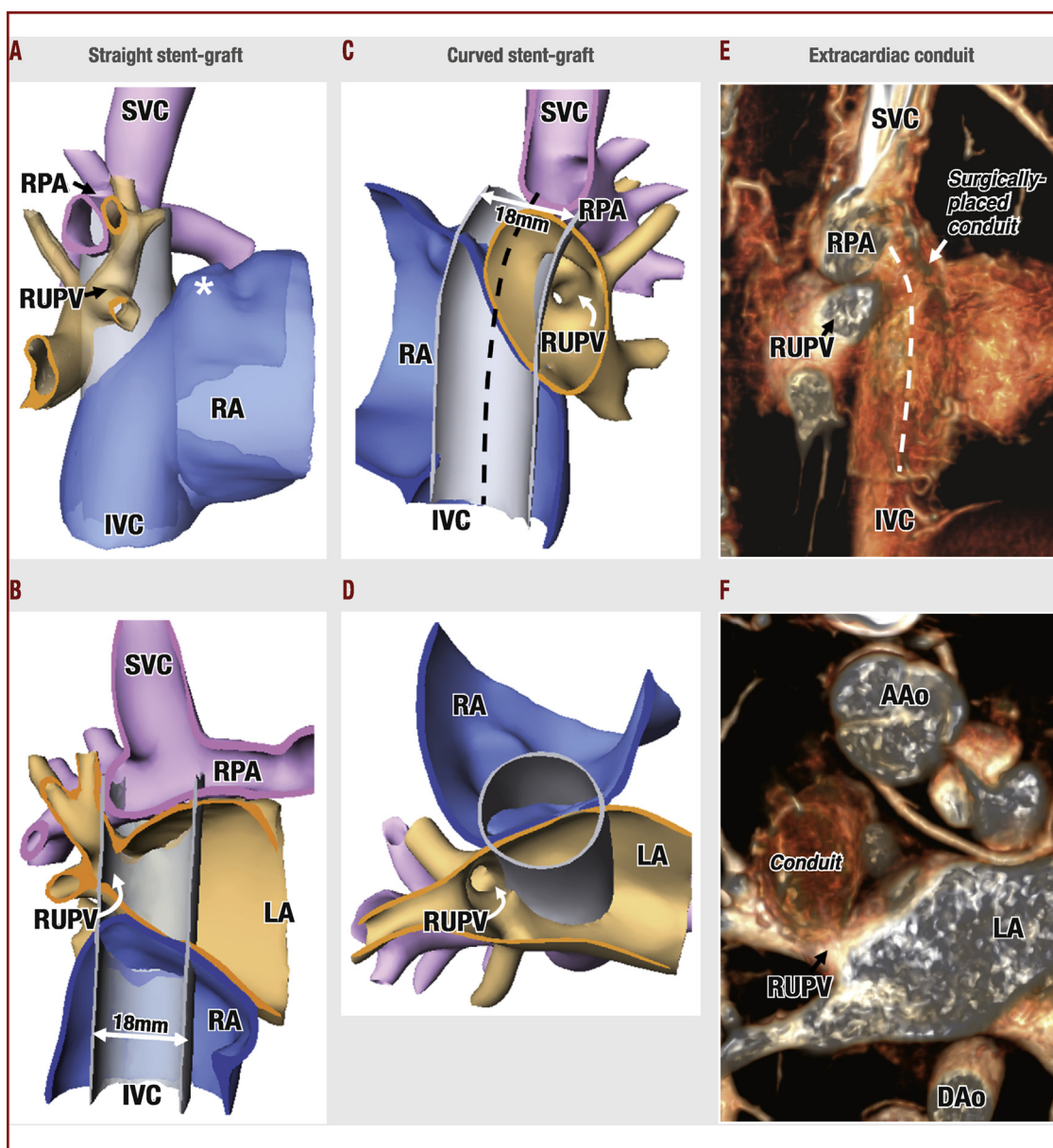


**Figure 4.** Spatial relationship between the atria, vessels and two types of superimposed covered stent-graft in a patient with representative challenging anatomy. Note the diameter discrepancy between the inferior vena cava (IVC), right pulmonary artery (RPA) and stent-graft. A, B. Straight covered 18 mm stent completely covering the right upper pulmonary vein (RUPV) orifice in this patient. Note the substantial gap between the RPA caudal surface and small cardiac stump of the superior vena cava (SVC; asterisk). C, D. Introduction of a slight curvature at the graft's cranial aspect allows IVC-to-RPA connection without covering the RUPV orifice. Note the displacement of the graft's longitudinal axis (dashed line) anterior to the RUPV. E and F. Right lateral and caudal views of the maximum intensity projections of the computed tomography angiogram performed in 8.5-year-old patient with extracardiac-type TCPC. Note the conduit's curvature (dashed line) and its "protrusion" into the adjacent atrium, anterior to the RUPV. Aao: ascending aorta; Dao: descending aorta; LA: left atrium; RA: right atrium.

Table 2 summarizes the results of calculations of the stent-graft dimensions using the measured distances. Large variability was observed in calculated lengths and shapes of the grafts among patients for whom a curved stent-graft would be necessary to avoid compromising the RUPV (Fig. 5A). There was no correlation between the measured RUPV-IVC distance and the upper arc length of the graft ( $r^2 < 0.01$ ;  $P = 0.87$ ), which produced a range of ~10–20 mm

of the graft's upper arc lengths per every given RUPV-IVC distance required to address the observed RUPV position variation (Fig. 5B). In contrast to unaltered upper arc length variability, fixation of the deviation value at 10 mm resulted in a substantially decreased variance in the graft's bend angle (Fig. 5C), corresponding to fewer device models per every given RUPV-RPA distance. At a fixed deviation, the graft's bend angle also became slightly sharper.

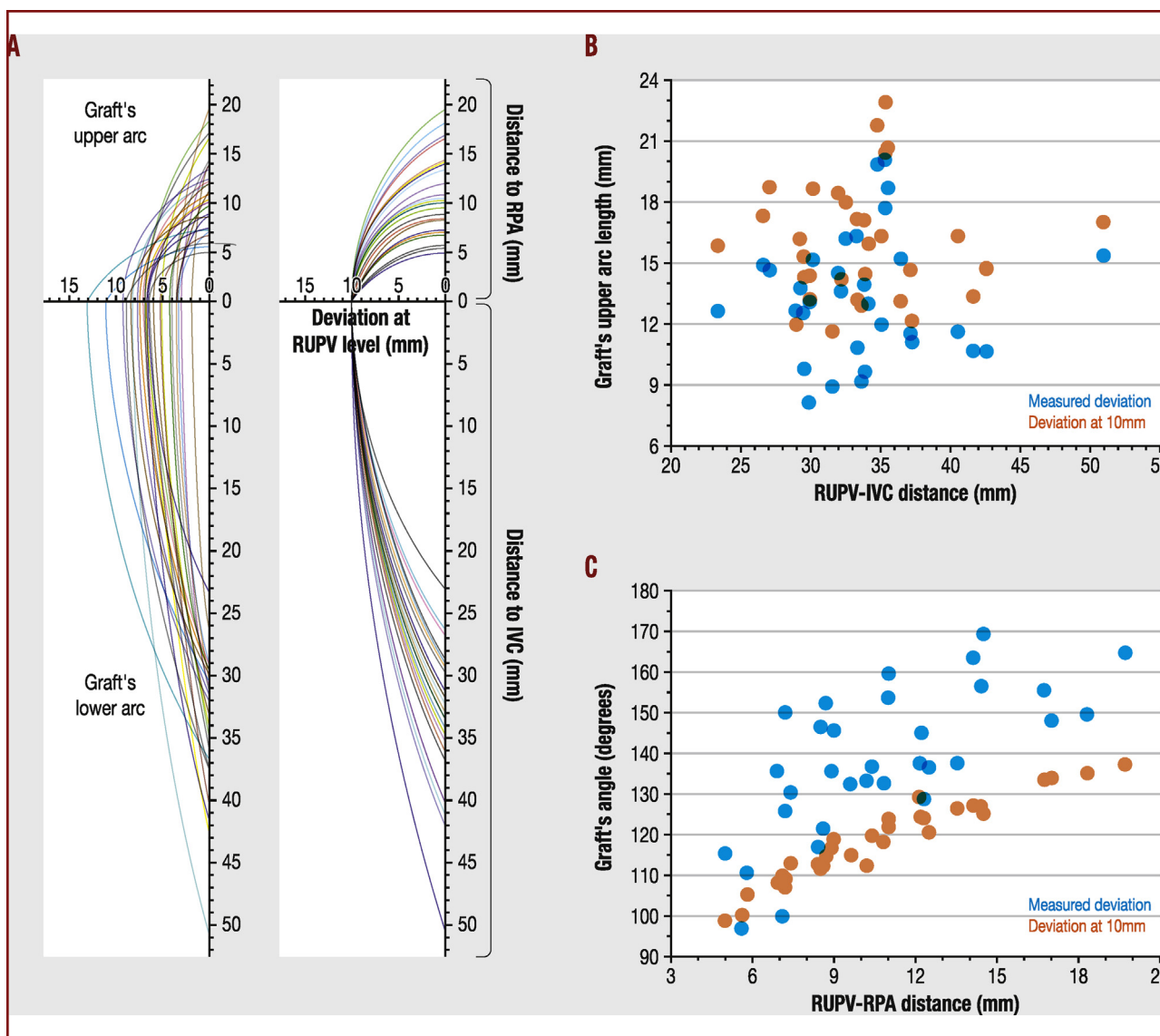


**Figure 5.** Centreline dimensions of the curved stent-graft to achieve TCPC completion in patients aged < 5 years, where a straight stent would compromise the right upper pulmonary vein (RUPV). A. Graphic presentation of the 32 individual centrelines of the curved stent-graft seen in the right-lateral view. The length and shape of the centrelines were calculated using the measured (left) and the fixed at 10 mm (right) values of the anterior deviation. B. Relationship between the RUPV-to-inferior vena cava (IVC) distance and the length of the graft's upper arc, demonstrating virtual absence of correlation between these two variables. C. Relationship between the RUPV-to-right pulmonary artery (RPA) distance and the graft's bend angle, showing a substantial decrease in the angle's variation when the deviation is fixed at 10 mm.

## Discussion

Transcatheter completion of the TCPC would shorten recovery time by reducing procedure invasiveness. Special surgical preparations seem to be necessary to facilitate transcatheter TCPC completion, with several modifications to the bidirectional Glenn anastomosis or hemi-Fontan procedures being proposed in the last 20 years [4–11]. In one approach, percutaneous TCPC completion was achieved by the intra-atrial IVC-to-SVC placement of straight balloon-expandable covered stents after perforation of a patch closing the distal SVC connected to the RPA during the Glenn procedure [5,6,9]. Appropriately-located fenestration in the covering of intra-atrial TCPC stent-graft was

then created using wire perforation followed by balloon dilatation.

Although providing certain advantages [13], surgical “preconditionings” of the cardiovascular anatomy for transcatheter TCPC completion have several drawbacks, being based on more-or-less extensive additional manipulations during the Glenn procedure in an infant. As result, transcatheter TCPC completion has not yet achieved acceptance, despite being a very attractive technique. Development of a dedicated TCPC completion device providing flow efficiency similar to a surgical conduit, and avoiding the necessity of “preconditionings” and addressing previously-encountered challenges, is necessary for this procedure to come back into clinical use. Systematic

evaluation of anatomical aspects regarding the design of such a dedicated device in children with conventional bidirectional Glenn anastomosis is presently lacking. With our study, we sought to fill this gap.

## Procedural considerations

Tight contact between the PA branch and adjacent atrial wall creates an attractive possibility to apply a technique of percutaneous intervascular anastomosis, which has been used successfully to create stent-secured TCPC fenestrations [14,15]. With the appropriate equipment, it would be possible to pass the perforation-wire from the RPA below the Glenn anastomosis directly into the adjacent atrial cavity in all our patients. Although essential to ensure optimal intra-atrial stent orientation, an SVC-to-IVC wire-loop results in device deployment that potentially eliminates haemodynamically-favourable off-set of the superior and inferior flows into the PAs. If proved true, this will necessitate alterations in either implantation technique or device design, to make the stent-secured TCPC completion haemodynamically more efficient.

A (nearly) intact atrial septum interposing between the IVC and Glenn anastomosis, which was present in 42% of our patients, may complicate intra-atrial graft deployment or creation of appropriately-located fenestration. This would necessitate creation of an atrial septal defect, which is relatively easily achievable percutaneously [16]. The presence of the cardiac SVC stump attached or in proximity to the RPA caudal surface, as was visible in 45% of our patients, is technically advantageous. Furthermore, transcatheter creation of the bidirectional Glenn anastomosis using a SVC-to-RPA covered stent will invariably leave the distal SVC attached to RPA wall, thus facilitating transcatheter TCPC completion at a later stage [17,18]. Avoiding hepatic vein obstruction by the IVC end of the stent-graft may be challenging, especially with the movement of organs as a result of respiration, and a relatively short landing zone, as was estimated in our patients. However, accurate graft placement can be facilitated by limiting organ and vessel motion through temporary suspension of mechanical lung ventilation during the procedure.

## Device design considerations

An ideal transcatheter TCPC completion device should provide haemodynamically-efficient and durable hermetic IVC-to-RPA communication, without compromising adjacent vessels or interfering with cardiac growth [13]. The capacity of the device to adapt to smaller RPA and larger IVC diameters, without reduction of the graft cross-sectional area, is equally important to avoid flow power loss or leakage within the TCPC circuit. Regular balloon-expandable straight covered stents placed between the venae cavae may protrude into the RPA lumen and compromise the RUPV, resulting in complications. Furthermore, dilation of the extremely compliant IVC may lead to insufficient sealing of the balloon-expandable stent, producing paraprosthetic leakage and important desaturation, requiring reinterventions [5,6].

In one-third of our patients, the average diameter of the distal IVC exceeded 20mm. In some surgical "preconditionings", the issue of IVC dilation beyond the

maximal size of the TCPC completion device was successfully addressed by placing pericardial strips or stents around the distal IVC [5,6,9]. The percutaneous creation of such a fixed landing zone within the IVC will be difficult. Alternatively, the active fixation feature of the stent-grafts, as currently used in endovascular repair of abdominal aortic aneurysms [19], with or without flaring of the end of the stent, can be used to secure and seal the device within the distal IVC, preventing it from further dilation. As we show here, a curved device, similar to the self-expanding curved stent-grafts used in endovascular repair of aortic arch aneurysms [20], will allow transcatheter TCPC completion without endangering the RUPV. The predicted position of such a curved intra-atrial stent-graft anterior to the RUPV closely resembles the bowed configuration of a surgically-placed extracardiac conduit (Fig. 4E and F).

In the children from our population aged <5 years, the RPA had a median diameter of only 12.2 mm, which is clearly too small to safely accommodate a round end of the stent completing the TCPC. Using the shape-memory feature of nitinol, the cranial end of the self-expanding stent-graft can easily be configured into an oval shape, allowing safe device deployment through the RPA wall without a decrease in the flow cross-sectional area. Moreover, the oval shape of the RPA end of the device will enable avoidance of compromise of the RUPV orifice in patients with a short RPA-RUPV distance. The issue of device protrusion into the RPA lumen can be successfully addressed using a trumpet-shaped design of the end of stent-graft, as recently demonstrated in a pig model of the stent-secured Glenn shunt [17]. Stent flaring within the RPA facilitates its apposition to the vascular inner surface, providing flow bidirectionality and minimizing protrusion.

Splitting the TCPC circuit flow into two curved streams is predicted to be haemodynamically beneficial [21]. Theoretically, there is intra-atrial space for a bifurcating covered stent similar to the device used in the endovascular treatment of distal abdominal aortic aneurysms [22]. Although such a bifurcating stent-graft would address the eventual flow collision after transcatheter TCPC completion, safe deployment of the Y-shaped end of such a device through the single perforation site in non-bifurcating atrial and RPA walls will be extremely difficult. Alternatively, nearly symmetrical four-way crossing of the inflows formed by the SVC and the stent-graft, and bidirectional outflow through PA branches, creates an ideal landing zone for a biconical cavopulmonary assist device based on von Karman's principle of a rotating viscous impeller pump, which simultaneously provides flow splitting and augmentation [23].

## Study limitations and unanswered questions

Our study population, selected based on the availability of specifically-timed cardiovascular imaging with sufficient anatomy visualization, although allowing comprehensive analysis regarding TCPC completion device design, does not accurately represent the average candidates who are suitable for this procedure, partially because of the high variability in age of the included patients. Additionally, this was a retrospective analysis of static imaging in patients where no transcatheter TCPC completion was performed. Although efforts were made to standardize the measurements,

an oblique nature of the cross-sectional planes resulted in relatively large intra- and interobserver variabilities.

Experimental studies are necessary to determine the optimal radial and longitudinal force necessary for the intended intra-atrial configuration of the self-expanding curved stent-graft upon deployment through the atrial and arterial walls, and to investigate whether distensibility of the atrial and distal SVC walls will be sufficient to accommodate such a device without damaging the sinus node. Flow evaluation through the curved stent-graft is also needed to assess flow turbulence and power loss compared with surgical TCPC [24].

## Conclusions

Our systematic analysis of cardiovascular anatomy and morphometry in a substantial number of children with univentricular heart defects provides important insights for further studies on transcatheter TCPC completion without surgical “preconditionings”. Regardless of the cardiovascular arrangement type, an intra-atrial curved stent-graft seems most suitable for the majority of children after conventional Glenn anastomosis, to achieve the Fontan completion percutaneously. Experimental study is necessary to validate this conclusion.

## Sources of funding

Financial support was provided by the Association pour la recherche en cardiologie du fœtus à l’adulte (ARCFA).

## Acknowledgements

The authors wish to thank the *Association pour la recherche en cardiologie du fœtus à l’adulte* (ARCFA) for financial support.

## Disclosure of interest

The authors declare that they have no competing interest.

## Appendix A. Supplementary data

Supplementary data associated with this article can be found, in the online version, at <https://doi.org/10.1016/j.acvd.2017.08.003>.

## References

- [1] Iyengar AJ, Winlaw DS, Galati JC, Celermajer DS, Wheaton GR, Gentles TL, et al. Trends in Fontan surgery and risk factors for early adverse outcomes after Fontan surgery: the Australia and New Zealand Fontan Registry experience. *J Thorac Cardiovasc Surg* 2014;148:566–75.
- [2] Salvin JW, Scheurer MA, Laussen PC, Mayer Jr JE, Del Nido PJ, Pigula FA, et al. Factors associated with prolonged recovery after the fontan operation. *Circulation* 2008;118:S171–6.
- [3] Ovroutski S, Sohn C, Miera O, Peters B, Alexi-Meskishvili V, Hetzer R, et al. Improved early postoperative outcome for extracardiac Fontan operation without cardiopulmonary bypass: a single-centre experience. *Eur J Cardiothorac Surg* 2013;43:952–7.
- [4] Boudjemline Y, Malekzadeh-Milani S, Van Steenberghe M, Bogli Y, Patel M, Gaudin R, et al. Novel method of surgical preparation for transcatheter completion of Fontan circulation: creation of an extracardiac pathway. *Arch Cardiovasc Dis* 2014;107:371–80.
- [5] Crystal MA, Yoo SJ, van Arsdell GS, et al. Catheter-based completion of the Fontan: a non-surgical approach. *Catheter Cardiovasc Interv* 2006;68:460 [abstract].
- [6] Galantowicz M, Cheatham JP. Fontan completion without surgery. *Semin Thorac Cardiovasc Surg Pediatr Card Surg Annu* 2004;7:48–55.
- [7] Hausdorf G, Schneider M, Konertz W. Surgical preconditioning and completion of total cavopulmonary connection by interventional cardiac catheterisation: a new concept. *Heart* 1996;75:403–9.
- [8] Klima U, Peters T, Peuster M, Hausdorf G, Haverich A. A novel technique for establishing total cavopulmonary connection: from surgical preconditioning to interventional completion. *J Thorac Cardiovasc Surg* 2000;120:1007–9.
- [9] Konstantinov IE, Benson LN, Caldarone CA, Li J, Shimizu M, Coles JG, et al. A simple surgical technique for interventional transcatheter completion of the total cavopulmonary connection. *J Thorac Cardiovasc Surg* 2005;129:210–2.
- [10] Metton O, Calvaruso D, Stos B, Ben Ali W, Boudjemline Y. A new surgical technique for transcatheter Fontan completion. *Eur J Cardiothorac Surg* 2011;39:81–5.
- [11] Sallehuddin A, Mesned A, Barakati M, Fayyadh MA, Fadley F, Al-Halees Z. Fontan completion without surgery. *Eur J Cardiothorac Surg* 2007;32:195–200 [discussion 1].
- [12] Konstantinov IE, Editorial comment. Transcatheter completion of Fontan circulation: primum non nocere! *Eur J Cardiothorac Surg* 2011;39:85–6.
- [13] Konstantinov IE, Alexi-Meskishvili VV. Intracardiac covered stent for transcatheter completion of the total cavopulmonary connection: anatomical, physiological and technical considerations. *Scand Cardiovasc J* 2006;40:71–5.
- [14] McMahon CJ, el-Said HG, Mullins CE. Transcatheter creation of an atriopulmonary communication in the Hemi-Fontan or Glenn circulation. *Cardiol Young* 2002;12:196–9.
- [15] Mehta C, Jones T, De Giovanni JV. Percutaneous transcatheter communication between the pulmonary artery and atrium following an extracardiac Fontan: an alternative approach to fenestration avoiding conduit perforation. *Catheter Cardiovasc Interv* 2008;71:936–9.
- [16] Veldtman GR, Norgard G, Wahlander H, Garty Y, Thabit O, McCrindle BW, et al. Creation and enlargement of atrial defects in congenital heart disease. *Pediatr Cardiol* 2005;26:162–8.
- [17] Ratnayaka K, Rogers T, Schenke WH, Mazal JR, Chen MY, Sonmez M, et al. Magnetic resonance imaging-guided transcatheter cavopulmonary shunt. *JACC Cardiovasc Interv* 2016;9:959–70.
- [18] Sizarov A, Raimondi F, Bonnet D, Boudjemline Y. Vascular anatomy in children with univentricular hearts regarding transcatheter bidirectional Glenn anastomosis. *Arch Cardiovasc Dis* 2017;110:223–33.
- [19] Donas KP, Kafetzakis A, Umscheid T, Tessarek J, Torsello G. Vascular endostapling: new concept for endovascular fixation of aortic stent-grafts. *J Endovasc Ther* 2008;15:499–503.
- [20] Sanada J, Matsui O, Terayama N, Kobayashi S, Minami T, Kurozumi M, et al. Clinical application of a curved nitinol stent-graft for thoracic aortic aneurysms. *J Endovasc Ther* 2003;10:20–8.

- [21] Marsden AL, Bernstein AJ, Reddy VM, Shadden SC, Spilker RL, Chan FP, et al. Evaluation of a novel Y-shaped extracardiac Fontan baffle using computational fluid dynamics. *J Thorac Cardiovasc Surg* 2009;137, 394–403 e2.
- [22] Qu L, Hetzel G, Raithel D. Seven years' single center experience of Powerlink unibody bifurcated endograft for endovascular aortic aneurysm repair. *J Cardiovasc Surg (Torino)* 2007;48:13–9.
- [23] Rodefeld MD, Coats B, Fisher T, Giridharan GA, Chen J, Brown JW, et al. Cavopulmonary assist for the univentricular Fontan circulation: von Karman viscous impeller pump. *J Thorac Cardiovasc Surg* 2010;140:529–36.
- [24] Hong H, Dur O, Zhang H, Zhu Z, Pekkan K, Liu J. Fontan conversion templates: patient-specific hemodynamic performance of the lateral tunnel versus the intraatrial conduit with fenestration. *Pediatr Cardiol* 2013;34:1447–54.